JOURNAL OF THE ROYAL SOCIETY Interface

MECHANICS OF PLANT FRUIT HOOKS

Journal:	*Journal of the Royal Society Interface*
Manuscript ID:	rsif-2012-0913.R1
Article Type:	Research
Date Submitted by the Author:	07-Jan-2013
Complete List of Authors:	Chen, Qiang; Southeast University, School of Biological Science and Medical Engineering Gorb, Stanislav; University of Kiel, Functional Morphology and Biomechanics Gorb, Elena; University of Kiel, Functional Morphology and Biomechanics Pugno, Nicola; Politecnico di Torino, Structural Engineering
Subject:	Biomechanics < CROSS-DISCIPLINARY SCIENCES, Biomaterials < CROSS-DISCIPLINARY SCIENCES
Keywords:	Plant Hooks, Force-displacement curves, Young's modulus, Velcro®

MECHANICS OF PLANT FRUIT HOOKS

Qiang Chen[1], Stanislav N. Gorb[2], Elena Gorb[2] and Nicola Pugno[3]*

[1]*Laboratory of Biomechanics, School of Biological Science and Medical Engineering, Southeast University, 210096, Nanjing, P.R. China.*

[2]*Functional Morphology and Biomechanics, University of Kiel, Am Botanischen Garten 1-9, D - 24098 Kiel, Germany, sgorb@zoologie.uni-kiel.de, egorb@zoologie.uni-kiel.de*

[3]*Department of Civil, Environmental and Mechanical Engineering, University of Trento, 38123 Trento, Italy.*

**Corresponding author: nicola.pugno@unito.it*

Revised Paper Submitted to J. R. Soc. Interface

Abstract. Hook-like surface structures, observed in some plant species, play an important role in the process of plant growth and seed dispersal. In this paper, we developed a geometrical model and further used it to investigate mechanical behavior of fruit hooks in four plant species, previously measured in the experimental study. Basing on Euler-Bernoulli beam theory, the force-displacement relationship is derived and Young's modulus is obtained. The result agrees well with the experimental data. The model aids in understanding an underlying mechanical mechanism of hook behavior, and could be used in the development of new bio-inspired Velcro®-like materials.

Keywords: Plant hooks, Force-displacement curves, Young's modulus, Velcro®.

1. INTRODUCTION

Recently studied hooks-like structures on different plant organs, which enhance their attachment ability, serve two main functions: (Ⅰ) to support stem in a densely-occupied environment [1] and (Ⅱ) to interlock with animal fur and feathers for fruit and seed dispersal [2]. To separate hooks from their supports, a strong force has to be applied.

Bauer et al. [1] have investigated the structure and mechanical properties of the climbing plant *Galium aparine*, which attaches to host plants using its leaves. In this experimental study, sets of tensile experiments were performed to estimate the contact separation force of single hooks in different load directions. Additionally, sliding friction of leaves was evaluated, to demonstrate difference in frictional properties between hooks situated on *abaxial* and *adaxial* sides of leaves. The authors found that differences in the hook position on the leaf surface, their orientations, shape, and sizes resulted in variable friction properties and pronounced friction anisotropy of both leaf side. Due to this, the plant can hold supports tightly and thus climb successfully to obtain more sunshine needed for photosynthesis.

On the surface of some fruits and seeds (later called *fruits*), hooks are involved in epizoochorous dispersal [2]. Such fruits can detach easily from their parental plants and attach to animals by interlocking with the animal hair or feathers. Using animals as vectors, they are carried to other places located at distances ranging from tens of meters to tens of kilometers [3, 4] from the parent plant. The dispersal distance depends on the particular animal vector, hook geometry, density of hooks, properties of hook material, and fruit mass. With such interesting phenomenon, recently, mechanical measurements on single hooks of *Geum urbanum*, *Agrimonia eupatoria*, *Galium aparine,* and *Circea lutetiana* were carried out [2] (figure 1). It was revealed that the hook

size and shape had a great influence on the contact separation force, generated by hooks during interlocking.

However, addressing how the material properties of fruit hooks influence their mechanical behavior, the relationship between them was not defined quantitatively in theory. In the present paper, we developed a geometrical model aiming at prediction of mechanical behaviors of the hooks. First, the entire hook geometry is subdivided into two parts; for each part, geometry was simplified and determined by several parameters taken from [2]. Second, Euler-Bernoulli beam theory was used to derive the force-displacement relationship and to predict Young's moduli of hook materials, which describes hook materials stiffness and is an important parameter in man-made hook fastener materials design.

2. MECHANICAL MEASUREMENTS ON SINGLE HOOKS

2.1 GEOMETRICAL DESCRIPTION OF HOOKS

Table 1 Geometrical parameters of hooks in four plant species (data from [2]). *N* denotes the number of hook samples

Geometrical	*A. eupatoria*			*C. luteriana*			*G. aparine*			*G. urbanum*		
Parameters	mean	SD	N	mean	SD	N	mean	SD	N	mean	SD	N
ls (µm)	1845.9	408.3	20	1066.1	272.8	20	281.1	42.1	20	4654.6	369.8	20
lh (µm)	94.3	13.3	20	87.2	40.9	20	19.6	4.8	20	235.0	34.1	20
dh (µm)	64.2	11.1	20	46.6	16.2	20	9.8	2.6	20	96.7	8.7	20
sh (µm)	90.9	20.9	20	173.6	60.3	20	29.6	11.8	20	220.3	29.0	20
dd (µm)	67.8	10.1	20	57.7	19.2	20	11.2	2.3	20	97.6	7.5	20
db (µm)	169.2	64.6	20	83.0	26.4	20	45.1	8.3	20	298.4	56.6	20
Hooks/fruit	73.7	10.2	10	182.1	24.7	6	183.3	27.2	8	1	0	50

Fruits of *A. eupatoria*, *C. lutetiana*, *G. aparine*, and *G. urbanum* were collected in Tübingen, (Germany) and examined using a light microscopy (Mitutoyo MF U-510 TH) in order to quantify the geometrical parameters of the hooks, such as the total length (*ls*), the diameter in basal (*db*) and distal parts (*dd*), the diameter (*dh*) and length of a curved part, hook, (*lh*) as well as its span

(*sh)*. These parameters together with the hook number per fruit are reported in Table 1 (data from [2]).

2.2 TESTING METHOD AND RESULTS

To study mechanical properties of fruit hooks, experiments were performed with individual hooks of each plant species. A single hook was cut off from the fresh fruits and its basal part was glued to a platform P using Universal glue GL (figure 2). The upper (curved) part of the hook was interlocked to a steel-wire loop LP with a diameter of 50 μm, which was attached to a glass spring G with a spring constant of 290 N m^{-1}. The hook slowly moved down driven by a motor on a force tester (Tetra GmbH, Ilmenau, Germany) during the experimental process until the contact between the hook and the loop was broken. The force tester included three main parts, a platform P, a glass spring G, and a fibre optical sensor FOS, which monitored the spring deflection by a mirror M, and was connected to a computer used for data acquisition (figure 2). The recorded force–displacement curves are presented in figure 3 (data from [2]).

It is found that the displacement is very large compared to the overall hook length. On the one hand, when the hook is subjected to a force, the pulling-straight effect contributes to the large deformation. On the other hand, because hook samples contain some residual water, their mechanical behaviors is rather ductile, thus, their deformations are large compared to the hooks' size. As for the sliding of the metal hook during testing, it has weak influence on the results obtained, since we have used only the linear part of the force-displacement curve.

Additionally, the number of burrs per fruit is in the approximate range from 73 for *A. eupatoria* for to 183 for *G. aparine* (table 1), thus, if the twist between hooks and animal hairs, which improves their interlocking effects, is not considered, the force required to detach a fruit

from an animal is from 646.1mN for *C. lutetiana* to 4511.4mN for *A. eupatoria* according to the breaking force in figure 3. The detaching force is much larger than the fruits' mass [2]. In biological sense, the dispersal distance relying on different hook geometry, density of hooks and properties of hook materials seems to be illustrated, even though the relevant data is still unavailable.

3. GEOMETRICAL MODEL OF THE HOOK

We used combinational curves to construct the hook model (figure 4a) according to the scanning electronic microscope (SEM) images in figure 1. The model is considered as a combination of two parts: a trapezoid cylinder with upper diameter *dd* and lower diameter *db* and a semi-circle on the top (see figure 4a). The plane section of the semi-circle is comprised of three circles sharing a center *O*, and their radii are denoted by R_1, R_2, R_3, respectively. The radii are determined by the hook span *sh* and the upper diameter *dd*, i.e. $R_1 = \frac{1}{2}(sh - \frac{1}{2}dd)$, $R_2 = \frac{1}{2}(sh + \frac{1}{2}dd)$ and $R_3 = \frac{1}{2}(sh + \frac{3}{2}dd)$. Here, we do not consider *lh* and *dh* in determining the radii, but they are used to calculated the length of the trapezoid cylinder, i.e. $ls - lh - dh$, where *lh* and *dh* are hook length and diameter of the middle part in the semi-circle, respectively. Basing on the model, we derive two important parameters by geometrical analyses, i.e. the cross-sectional radii of the two parts, which determine the cross-sectional properties, e.g. moment of inertia. For the trapezoid cylinder, the radius is expressed as $r_1(y) = \frac{dd}{2}(1 + Py)$ with $P = \frac{1 - db/dd}{ls - lh - dh}$. For the semi-circle, we assume that cross sections are uniform with a diameter *dd*; thus, we derive the following radius: $r_2(\theta) = \frac{dd}{2}$. Using our basic model of hooks and mean geometrical parameters listed in Table 1, the four geometrical models for hooks of the four plant species can be obtained.

4. DISPLACEMENT OF THE HOOK

If the interaction between the hook and animal hair or feather is strong, fruits could be dropped at a more remote place. The information on the mechanical properties of hook materials is necessary to better understand the underlying dispersal mechanism. In the following sections, the Euler-Bernoulli beam theory was employed to calculate hook mechanics.

4.1 Trapezoid cylinder part

For the trapezoid cylinder part (figure 4a), the displacement includes the axial displacement $u_1(y)$, induced by the axial force *F*, which contacts with the top of the inner semi-circle with radius R_1. The horizontal displacement $w_1(y)$ is imposed by the bending moment $M_1(y) = -FR_2$, which is considered as a constant during the hook deformation. Neglecting the axial compliance and thus displacement $u_1(y)$, the displacement $w_1(y)$ must satisfy the classical elastic line equation:

$$\frac{d^2 w_1(y)}{dy^2} = -\frac{M_1(y)}{EI(y)} = \frac{4FR_2}{\pi E} \cdot \frac{1}{r_1(y)^4} \tag{1}$$

Substituting $r_1(y)$ into Eq. (1) and integrating it with boundary conditions $w_1'(-(ls - lh - dh)) = 0$, $w_1(-(ls - lh - dh)) = 0$, we have:

$$\begin{aligned} w_1'(y) &= -\frac{64FR_2}{3\pi EPdd^4} \cdot \left[\frac{1}{(1+Py)^3} - \left(\frac{dd}{db} \right)^3 \right] \\ w_1(y) &= -\frac{32FR_2}{3\pi EP^2 dd^4} \cdot \left[-\frac{1}{(1+Py)^2} - 2\left(\frac{dd}{db} \right)^3 (1+Py) + 3\left(\frac{dd}{db} \right)^2 \right] \end{aligned} \tag{2}$$

In the case of $y = 0$, we can find the rotation angle $\alpha = w_1'(0)$ and the horizontal displacement $w_1(0)$ at the distal end, i.e.,

$$\alpha = w_1'(0) = -\frac{64FR_2}{3\pi EPdd^4}\cdot\left[1-\left(\frac{dd}{db}\right)^3\right]$$

$$w_1(0) = -\frac{32FR_2}{3\pi EP^2dd^4}\cdot\left[-1+3\left(\frac{dd}{db}\right)^2-2\left(\frac{dd}{db}\right)^3\right]$$

4.2 Semi-circle part

In this part (figure 4a), we decompose the displacement into two steps: one is the rigid displacement, caused by both the rotation and translation of the distal end, and the other one is deformation displacement (figure 4b). Note that displacement trajectory of the hook tip resembles the centroid line (dashed line in figure 4a).

Rigid movement

In the case of the rigid movement, the semi-circle moves to the position Ⅱ from its original position Ⅰ. In the position Ⅱ, the coordinate vector of the semi-circle is expressed as:

$$\vec{r}_{\text{II}} = N\vec{r}_1 + \vec{w}_1 \tag{3}$$

with

$$N = \begin{bmatrix} \cos\alpha & \sin\alpha \\ -\sin\alpha & \cos\alpha \end{bmatrix}$$

$$\vec{r}_1 = (-R_2 + R_2\cos\theta, R_2\sin\theta)^T$$

$$\vec{w}_1 = (w_1(0), 0)^T$$

where $\vec{r}_1$ is the original position vector, $\vec{w}_1$ is the translational vector of the coordinate transformation, N is the rotation matrix of the coordinate transformation. Correspondingly, due to the rigid movement, the point, on which the applied force F acts, maintains the same rotation angle α from its original position: at the beginning, the force F acts on the semi-circle at the point with an angle coordinate of θ_0 =90°, and the coordinate vector is expressed as $(X_0, Y_0) = (-R_2 + R_2\cos\theta_0, R_2\sin\theta_0)$.

Deformation displacement

The displacement $v(\theta)$ can be calculated in the same way as that in the Section 3.1, but the coordinate should be replaced by the arc length *s*, which is the function of θ (i.e., $s = \theta R_2$) [5]. The moment $M_2(\theta)$ acting on the arc part is expressed as $M_2(\theta) = -F\left[\vec{r}_{\text{II}}(\theta) - \vec{r}_{\text{II}}(\theta_0 + \alpha)\right] \cdot \vec{\text{e}}_x$, when $\theta < \theta_0 + \alpha$, where $\vec{\text{e}}_x = (1,0)^T$ is the unit vector along the *x* axis. Thus, the displacement is expressed as:

$$\frac{d^2v(\theta)}{ds^2} = \frac{d^2v(\theta)}{R_2^2 d\theta^2} = -\frac{M_2(\theta)}{EI(\theta)} = \frac{4FR_2}{\pi E} \cdot \frac{\cos(\theta - \alpha)}{r_2(\theta)^4} \tag{4}$$

Plugging $r_2(\theta)$ into Eq. (4), we obtain:

$$\frac{d^2v(\theta)}{d\theta^2} = \frac{64FR_2^3}{\pi Edd^4} \cdot \cos(\theta - \alpha) \tag{5}$$

Integrating Eq. (5) with boundary conditions $v'(0) = 0$ and $v(0) = 0$, we obtain the expressions of cross-section rotation angle and displacement as:

$$\begin{aligned} v'(\theta) &= \frac{64FR_2^3}{\pi Edd^4} \cdot \left[\sin(\theta - \alpha) + \sin\alpha\right] \\ v(\theta) &= \frac{64FR_2^3}{\pi Edd^4} \cdot \left[-\cos(\theta - \alpha) + \theta\sin\alpha + \cos\alpha\right] \end{aligned} \tag{6}$$

Furthermore, the deformation displacement vector is $\vec{v} = (v(\theta)\cos(\theta - \alpha), v(\theta)\sin(\theta - \alpha))^T$. Thus, the final position coordinate of the semi-circle part can be determined as:

$$\vec{r}_{\text{III}} = \begin{cases} \vec{r}_{\text{II}} + \vec{v} & \text{if } \theta < \theta_0 + \alpha \\ \vec{r}_{\text{II}} + \vec{v}(\theta_0 + \alpha) & \text{if } \theta > \theta_0 + \alpha \end{cases} \tag{7}$$

In particular, for the part $\theta < \theta_0 + \alpha$, the new position in the coordinate is expressed as:

$$\begin{cases} X(\theta) = -R_2\cos\alpha + R_2\cos(\theta - \alpha) + w_1(0) + v(\theta)\cos(\theta - \alpha) \\ Y(\theta) = R_2\sin\alpha + R_2\sin(\theta - \alpha) + v(\theta)\sin(\theta - \alpha) \end{cases} \tag{8}$$

5. FORCE-DISPLACEMENT RELATIONSHIP

Comparing the positions before and after deformation of the points, on which the external force is applied, the total displacement experienced by the force *F* can be described by two

components under the conditions of $\theta_0 = 90^\circ$ and $(X_0, Y_0) = (-R_2 + R_2\cos\theta_0, R_2\sin\theta_0)$:

$$\begin{cases} \Delta_x = X(\theta_0+\alpha) - X_0 = -R_2\cos\alpha + w_1(0) + R_2 \\ \Delta_y = Y(\theta_0+\alpha) - Y_0 = R_2\sin\alpha + v(\theta_0+\alpha) \end{cases} \quad (9)$$

5.1 Comparison between experimental and prediction force-displacement curves

Employing the above equation (i.e. equation (9)), the theoretical force-displacement curves of hooks of the four plant species are obtained by fitting the experimental curves (figure 5). These curves reflect the typical constitutive behaviors of plant hooks. We found that the relationships are almost linear and are consistent with the experimental curves obtained by the same experimental design but used in estimating the ultimate load [6]. From these fits, Young's moduli were predicted (figure 6a). By taking the *A. eupatoria* hook as an example, we plotted the deformation, when the external force *F* equals 20mN (figure 6b).

Values of the Young's moduli obtained for four plant species studies are comparable to those reported for the grass hedge stems (2.6-8.5 GPa) [7], lignin (2.0 GPa) [8] and plant cell wall (7.0-15.0 GPa) [9]. The Young's modulus of the *G. aparine* hook is the highest (≈9.5 GPa) (figure 6a) and corresponds well to the range of values 2.02-23.2 GPa, previously calculated for different individual hooks of this plant species [6]. The Young's modulus of the *C. luteriana* hook is the lowest among plant species studied (figure 6a). This also verifies previous experimental results [2]: although the size of the *G. aparine* hooks was the smallest, the load at contact separation was larger than that of *C. luteriana* (figure 3). The latter has a lower material stiffness, which induces a slip off instead of hook fracture observed previously [2]. Compared with *G. aparine*, the *G. urbanum* hook has a lower Young's modulus (figure 6a), but a relative high load at contact separation (figure 3). This may be interpreted due to the larger size of *G. urbanum* hooks.

5.2 Mechanical behaviors of hooks

It is worth saying that the composite structure and material properties of fruit hooks were previously studied only in the *Galium aparine*. Staining of resin-embedded semithin sections with safranin and fast green showed that the hook wall contains cellulose and lignin [6]. Using force-distance curves obtained in contact separation experiments [2,6], Young's moduli of the hooks with and without a base were calculated in different way. Moreover, hooks with and without the base showed significantly different values of the elastic moduli: 2.02 GPa and 23.20 GPa, respectively ($H=755.44$, $df=1$, $P<0.001$, Kruskal-Wallis one-way ANOVA on ranks).

Moreover, from the viewpoint of mechanical design, in order to construct a desirable hook-based fastening device, it would be of importance to know how geometrical parameters of hooks influence mechanical behaviour of hooks independently of materials composition. Therefore, we studied four parameters, namely, the hook length (*ls*), hook span (*lh*), the diameter in distal end (*dd*) and the diameter in basal end (*db*), respectively, basing on the data obtained for *G. urbanum* hooks. The results of such an analytical study, where one of the geometrical parameters was varied and the others were kept constant, are reported in figure 8. We can see that increasing hook length (*ls*) and hook span (*lh*) results in a greater displacement under identical external forces, which indicates a more compliant hook; while under identical external forces, increasing diameter in distal end (*dd*) and diameter in basal end (*db*) produces a smaller displacement, which suggests a stiffer hook.

6. CONCLUSION

We have developed a theoretical model aimed to explain the mechanical behavior of the plant hooks and to obtain the force-displacement relationship, degree of the hook deformation, and

Young's modulus. The influences on the mechanical behavior of hooks are discussed and thus, the present theory can be potentially used for understanding mechanics of natural hooks and related structures. Additionally, the model could help in designing of new bio-inspired Velcro®-like mechanical adhesives [5, 6,10].

ACKNOWLEDGEMENTS

The research related to these results has received funding from the European Research Council under the European Union's Seventh Framework Programme (FP7/2007–2013)/ERC Grant agreement nu [279985] (ERC StG Ideas 2011 BIHSNAM on ''Bio-inspired hierarchical super nanomaterials'') to NP. The second and third author was supported by the German Science Foundation (grant C10 within the DFG SFB 677 "Function by switching" to SNG). This study was partly supported by the SPP 1420 priority program of the German Science Foundation (DFG) 'Biomimetic Materials Research: Functionality by Hierarchical Structuring of Materials' (project GO 995/9-2) to SG

REFERENCES

1 Bauer, G., Klein, M.-C., Gorb, S. N., Speck, T., Voigt, D. & Gallenmüller, F. 2011 Always on the bright side: The climbing mechanism of *Galium aparine*. *Proc. R. Soc. B* **278**, 2233-2239. (doi: 10.1098/rspb.2010.2038)

2 Gorb, E. & Gorb, S. 2002 Contact separation force of the fruit burrs in four plant species adapted to dispersal by mechanical interlocking. *Plant Physiol. Biochem.* **40**, 373-381. (doi:10.1016/S0981-9428(02)01381-5)

3 Howe, H. F. & Smallwood, J. 1982 Ecology of seed dispersal. *Ann. Rev. Ecol. Syst.* **13**, 201-228. (doi: 10.1146/annurev.es.13.110182.001221)

4 Manzano, P. & Malo, J. E. 2006 Extreme long-distance seed dispersal via sheep. *Front Ecol. Environ*. **4**, 244-248. (doi: 10.1890/1540-9295(2006)004[0244:ELSDVS]2.0.CO;2)

5 Pugno, N. M. 2007 Velcro® nonlinear mechanics. *Appl. Phys. Lett.* **90**, 121918. (doi: 10.1063/1.2715478)

6 Gorb, E. V., Popov, V. L. & Gorb, S. N. 2002 Natural hook-and-loop fasteners: anatomy, mechanical properties, and attachment force of the jointed hooks of the *Galium aparine* fruit. In *Design and Nature*: *Comparing Design in Nature with Science and Engineering* (eds. C. A. Brebbia, L. J. Sucharov, P. Pascolo), pp. 151-160. Southampton and Boston: WIT Press.

7 Dunn, G. H. & Dabney, S. M. 1996 Modulus of elasticity and moment of inertia of grass hedge stems. *Trans. ASAE.* **39**, 947-952.

8 Cousions, W. J. 1976 Elastic modulus of lignin as related to moisture content. *Wood. Sci. Technol.* **10**, 9-17. (doi: 10.1007/BF00376380).

9 Tashiro, K. & Kobayashi, M. 1991 Theoretical evaluation of three-dimensional elastic constants

of native and regenerated cellulose: role hydrogen bonds. *Polymer* **32**, 1516-1526. (doi: 10.1016/0032-3861(91)90435-L).

10 Pugno, N. 2008 Spiderman gloves. *Nano Today* **3**, 35-41. (doi: 10.1016/S1748-0132(08)70063-X).

Figure Captions:

Figure 1. Fruit hooks of four plant species: (a) *G. urbanum*, (b) *A. eupatoria*, (c) *G. aparine*, (d) *C. lutetiana*. *Permission pending from* [2]. (Copyright 2002 Elsevier)

Figure 2 Schematic of force tester. B, FOS G, GL, LP, M and P indicate hook, fibre optical sensor, glass spring, glue, steel-wire loop, mirror and platform, respectively. *Permission pending from* [2]. (Copyright 2002 Elsevier)

Figure 3 Force-displacement curves measures for single hooks of four plant species. Data from [2]. Note: A, B, C and D are separation points of the hooks, when the critical forces arrive. A. eu, C. lu, G. ap, G. ur indicate *A. eupatoria, C. lutetiana, G. aparine, G. urbanum*, respectively.

Figure 4. Schematic of hooks: (a) Geometrical model; (b) Deformation under tensile load. See sections 2.1 and 3 for abbreviations in (a) and section 5 for abbreviations in (b).

Figure 5. Comparison between experimental and theoretical force-displacement curves for hooks of the four plant species. Red lines are theoretical results. Blue lines are experimental results. Data from [2].

Figure 6. (a) Theoretically estimated Young's moduli for different hooks. (b) Model of the hook deformation in *A. eupatoria* at the applied load of F=20 mN. Blue line denotes the deformed configuration of the hook. Red line indicates the initial (not-deformed) configuration of the hook. A. eu, C. lu, G. ap, G. ur are *A. eupatoria, C. lutetiana, G. aparine, G. urbanum*, respectively.

Figure 7. Influences of geometrical parameters on the mechanical behavior of hooks. (a) influence of *lh*, which reflects the hook span; (b) influence of hook length *ls*; (b) influence of the diameter in distal end *dd*; (b) influence of the diameter in basal end *db*.

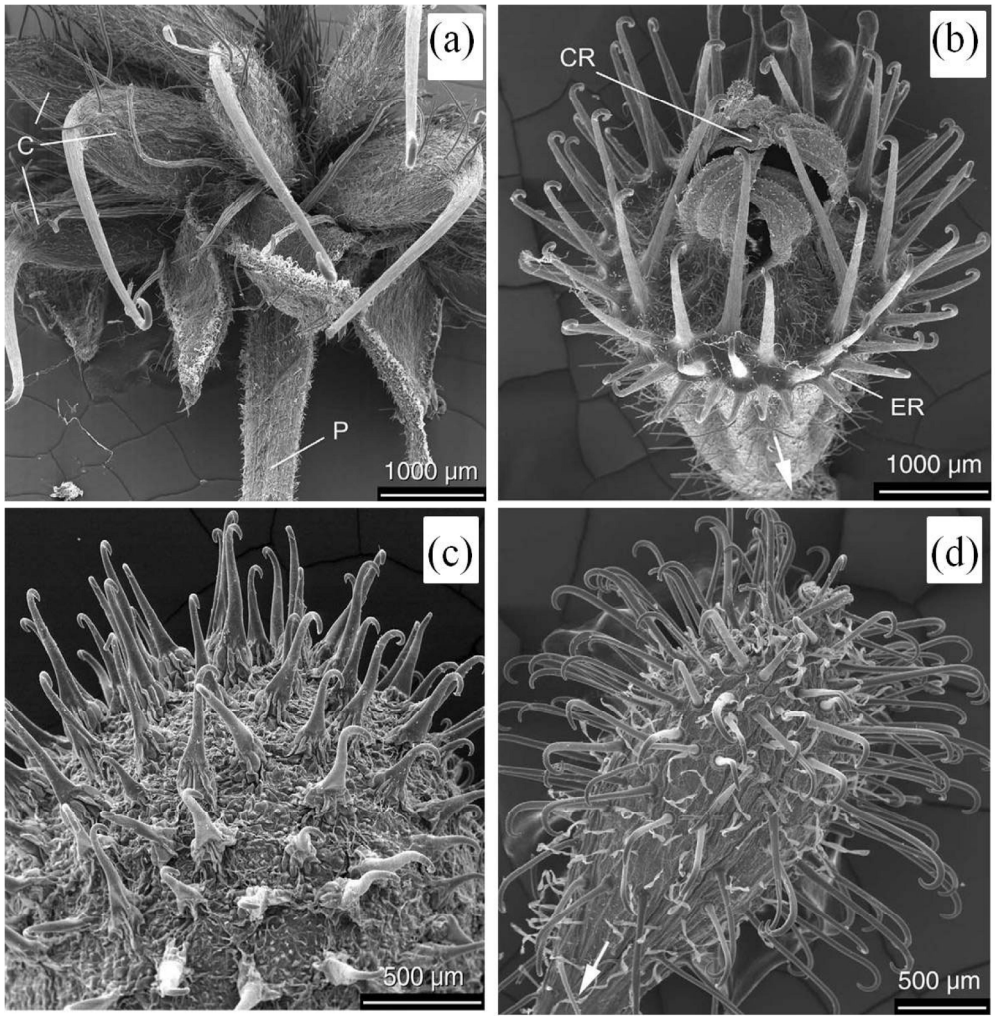

205x208mm (300 x 300 DPI)

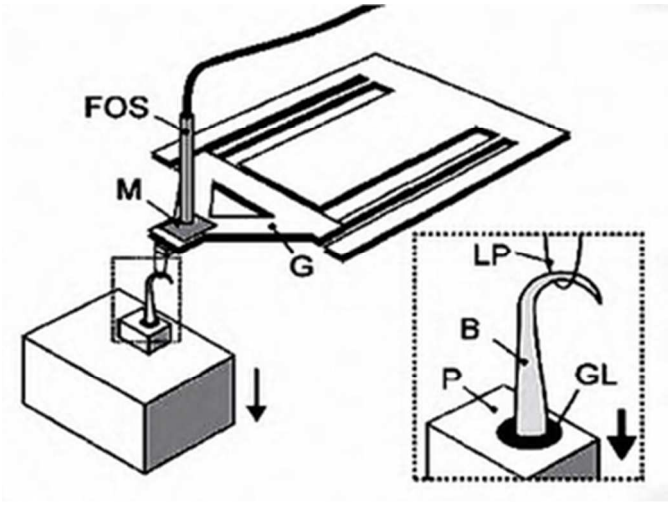

28x20mm (300 x 300 DPI)

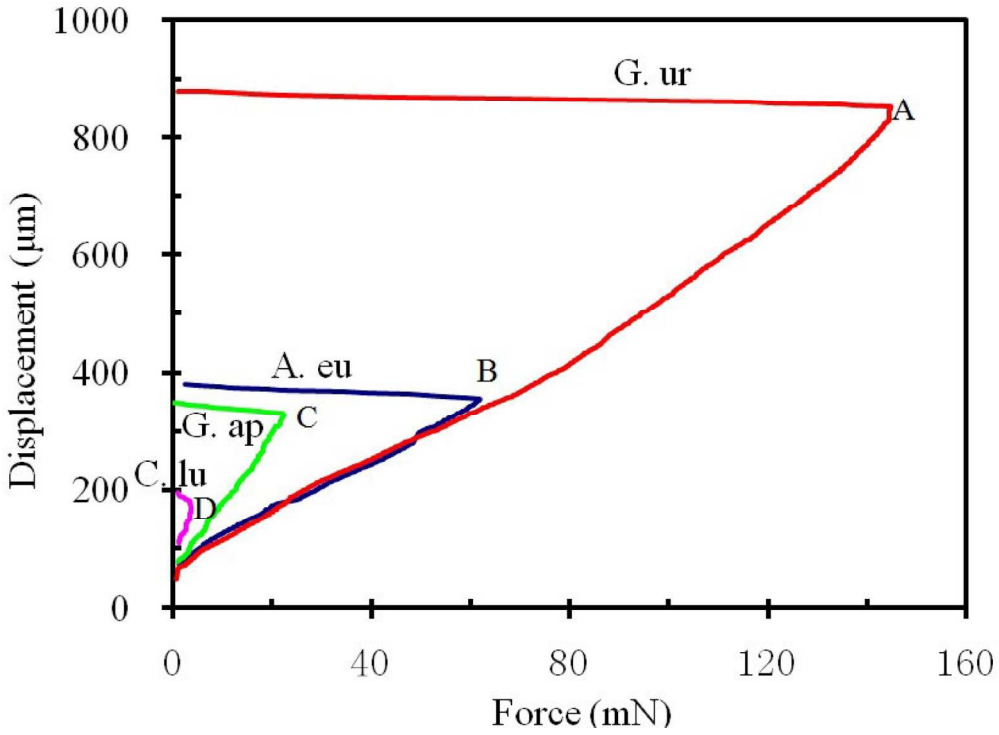

158x115mm (300 x 300 DPI)

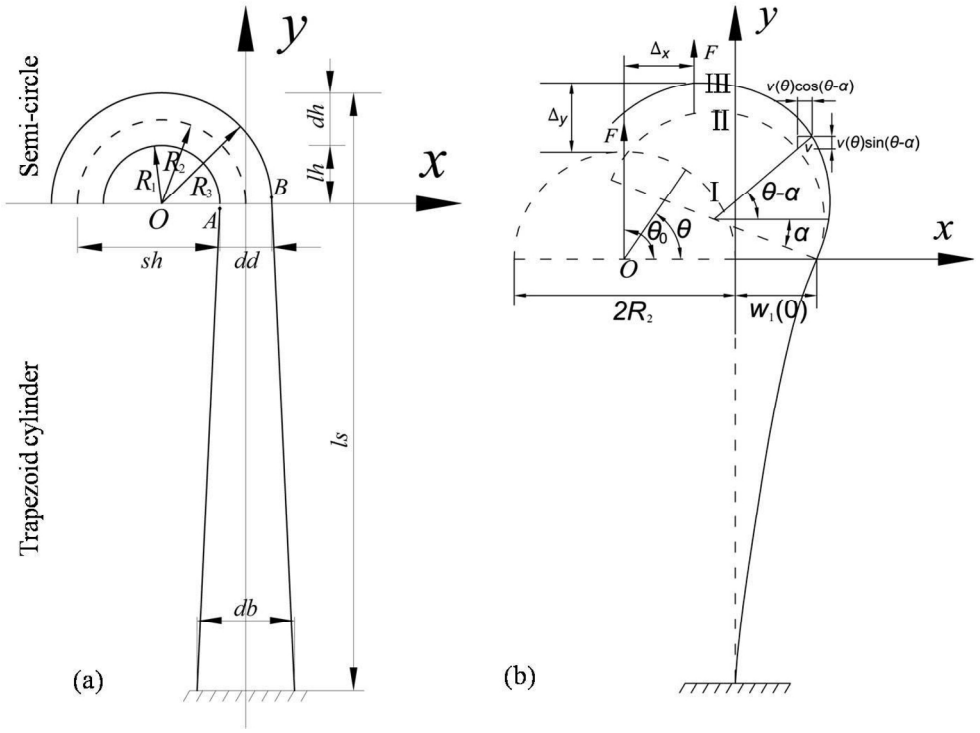

182x136mm (300 x 300 DPI)

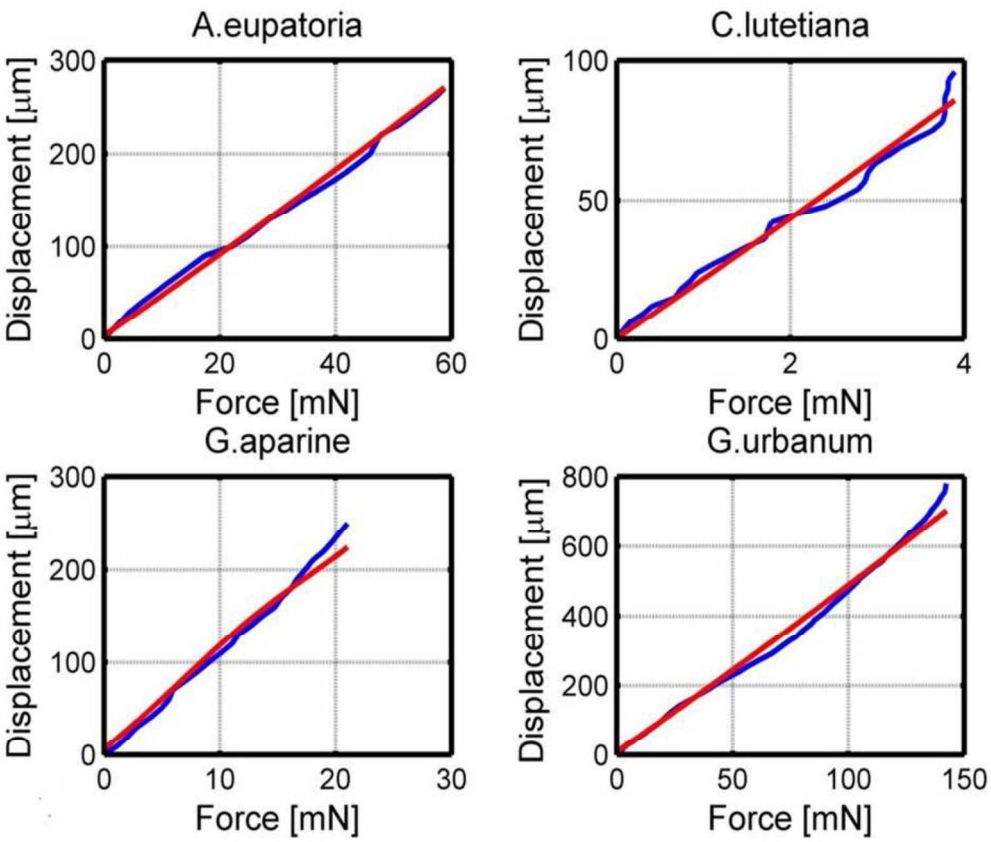

134x113mm (300 x 300 DPI)

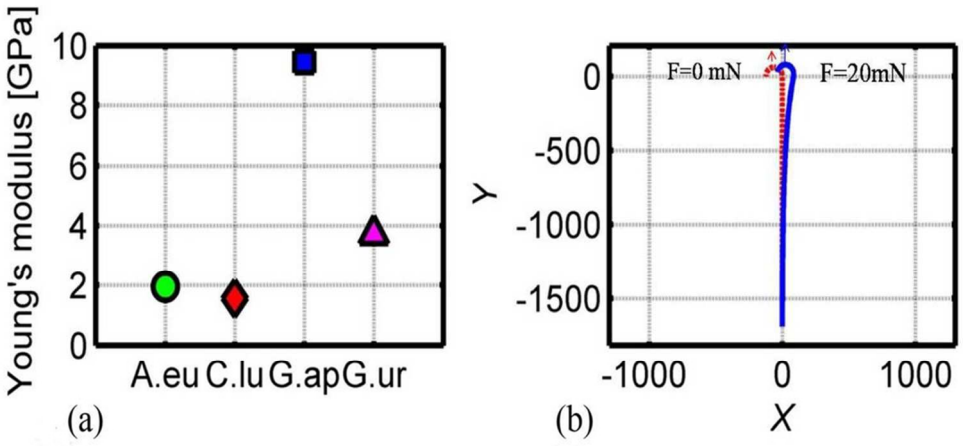

93x42mm (300 x 300 DPI)

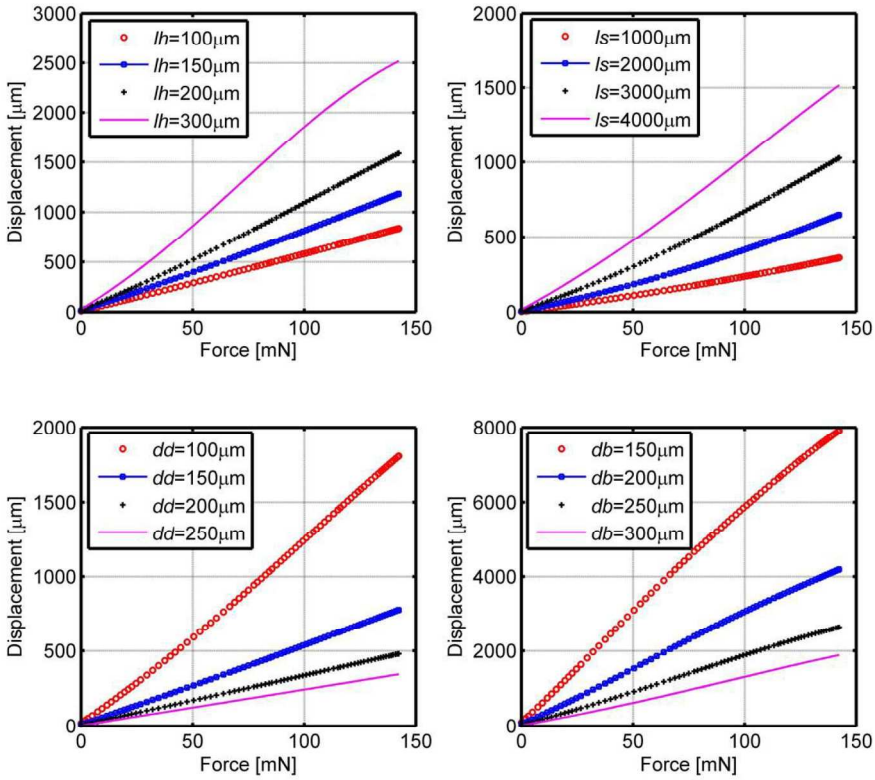

190x167mm (300 x 300 DPI)